RESEARCH ARTICLE

Editorial Process: Submission:07/10/2024 Acceptance:11/07/2024

Comparative Analysis of Dose Gradients and Valley Doses in Pelvic Lattice Radiotherapy in RapidArc and IMRT

Bhagyalakshmi AT[1,2], Velayudham Ramasubramanian[1]*

Abstract

Purpose: This study evaluated the dose fall off and valley dose percentage in pelvic cancer Lattice Radiotherapy (LRT) using various treatment techniques. **Methods:** Forty five treatment plans were developed for 15 patients undergoing radiotherapy using a linear accelerator. Plans were categorized into three sets: RapidArc (RA), seven-field intensity-modulated radiation therapy (IMRT), and nine-field IMRT, both for high-dose (HD) vertices and the entire planning target volume (PTV). Dose fall-off indices were analyzed using the normalized dose fall-off index (ʌ) to compare the rate of dose decrease beyond HD vertices. Valley dose percentages were determined by analyzing dose profiles between HD vertices to quantify lower dose percentages. Analysis involved averaging normalized dose fall-off index (ʌ) values, valley dose percentages and grouping valley doses to assess variation with respect to center-to-center (CTC) intervals between HD vertices for all the techniques. **Results:** RA plans achieved sharper dose fall-off beyond HD vertices compared to seven-field and nine-field IMRT techniques, with decreasing values as distance from the central plane increased. RA plans also exhibited higher valley doses (62.05%) relative to nine-field IMRT (55.02%) and seven-field IMRT (56.56%) for an average CTC distance of 3.75 cm, showing significant variability across CTC intervals. **Conclusions:** RA plans achieve steeper dose fall-off and higher valley doses compared to IMRT, effective for pelvic LRT but less suitable for grid therapy due to challenges with MLCs. Minimal differences in valley doses between nine-field and seven-field IMRT suggest limited impact from beam angles, guiding treatment optimization. The equations derived can be utilized for dosimetric evaluation and clinical planning in grid therapy, emphasizing their practical relevance in treatment strategy development.

Keywords: Dose fall off index- peak dose- valley dose- lattice therapy- high dose vertices

Asian Pac J Cancer Prev, **25 (11)**, 4061-4066

Introduction

Lattice Radiotherapy (LRT) is a form of Spatially Fractionated Radiotherapy (SFRT) that combines conventional dose fractionation regimens with the ablative nature of grid therapy [1, 2]. According to the literature, grid therapy using high dose is implemented in bulky, hypoxic tumors that are essentially inoperable, particularly in cases where the vascularity within the tumor cells is so minimal that it becomes undetectable to systemic chemotherapeutic drugs [3]. The therapeutic advantage of grid therapy has been demonstrated to be superior to conventional therapy in the treatment of bulky tumors [4]. In LRT, the treatment plans are created in a way that there are a series of spherical or near-spherical high dose (HD) vertices within the Gross Tumor Volume (GTV) prescribed with high doses for three to five fractions, and the valleys made up of the remaining Planning Target Volume (PTV) prescribed with a conventional dose using conventional fractionation [1]. High-dose LRT can result in a significant reduction in tumor volume, transcending the effects expected from homogeneous dose delivery. This reduction appears to be mediated by interactions between irradiated tumor cells and nearby unirradiated cells or those receiving a low radiation dose. The signaling from irradiated cancer cells may trigger tumoricidal effects in adjacent unirradiated tumor subvolumes through the bystander effect and in distant metastases through the abscopal effect [5, 6]. In grid therapy, the minimum valley dose could be as low as 25% of the prescription dose, while doses lesser than nearly 50% and higher than 120% were respectively observed beyond and at the proximal areas of bulky tumors. With the advent of multileaf collimators (MLCs) and intensity-modulated radiotherapy techniques, substantial dose reduction in the peripheral areas was accomplished [7]. However, the dose in valleys increased due to inter-leaf and intra-leaf transmission through MLCs and with the use of multiple angles for dose delivery [2]. In this study, we analyzed the dose fall-off and valley dose percentage for LRT using various techniques, including Rapid Arc (RA), seven-field IMRT, and nine-field IMRT. This data is crucial for determining the appropriate

*[1]School of Advanced Sciences, Vellore Institute of Technology, Vellore, India. [2]Department of Radiation Oncology, American Oncology Institute, Kozhikode, India. *For Correspondence: vrsramasubramanian@gmail.com*

prescription dose and its effective clinical application. A high valley dose percentage can result in cascading tissue damage, undermining the goal of reduced toxicity, while dose fall-off plays an important role in better sparing of organs at risks.

Materials and Methods

The study included forty-five plans for a cohort of 15 patients who underwent radiotherapy using a 6 MV beam from a Varian Clinac iX linear accelerator. To evaluate the dose fall off index and valley dose percentage in the context of lattice therapy for pelvic cancer patients with extensive disease, Computed Tomography (CT) slices with a thickness of 2.5 mm were acquired from a 16-slice Discovery IQ3 ring Positron Emission Tomography (PET) CT machine manufactured by Wipro GE.

The planning volume (PTV) in this study varied from 1389.6 cubic centimeters (cc) to 1649.9cc. The split of cases were five patients with bladder cancer, five patients with rectum cancer and five patients with advanced stage prostate cancers. Contouring of the HD vertices, GTV, PTV and other relevant normal structures was performed using the Varian SomaVision contouring station version 16.1. Eight small spherical vertices with an average diameter of 1.3cm and center to center (CTC) spacing of 3.75cm were contoured by optimizing the position of HD vertices within the GTV of each patient, while maximally avoiding the slices of organs at risk (OARs). These small HD regions within the GTV were prescribed an additional simultaneously integrated high dose of 27 Gy delivered in three fractions, alongside the conventional fractionated dose of 50Gy in 25 fractions for the entire PTV for bladder cases, 50.4 Gy in 28 fractions for rectum cases and 30Gy in 10 fractions for prostate cases. All treatment plans were generated specifically for this study at a single isocenter using 6 MV beams in the Eclipse treatment planning system(Varian). Three sets of plans were created in all the patients to quantify both dose fall of index and valley dose percentage. The first set consisted of a rapid arc (RA) plan for the HD vertices and another RA plan was created for the entire PTV. The second set involved a seven-field IMRT plan for the HD vertices and a separate seven-field IMRT plan for the entire PTV. Finally, the third set comprised a nine-field IMRT plan for the HD vertices and another nine-field IMRT plan for the entire PTV. Two complete arcs were chosen for the RA plans: one with a gantry start angle of 181° and ending at 179° clockwise, and the other with a start angle of 179° and ending at 181° counterclockwise. Additionally, two non-coplanar half arcs were selected: one with gantry rotation starting from 90° to 270° and a couch angle of 30°, and another with gantry rotation starting from 270° to 90° with the couch rotated to 330°. Meanwhile, seven equally spaced fields with gantry angles of 0°, 51°, 102°, 153°, 204°, 255°, and 306° were chosen as field arrangements for the seven-field IMRT plans. Similarly, nine equally spaced fields with gantry angles of 0°, 40°, 80°, 120°, 160°, 200°, 240°, 280°, and 320° were chosen as the field arrangements for the nine-field IMRT plans. The dose rates were 600 MU/min for the arc plans and 400 MU/min for the IMRT plans. The same set of arc/field arrangements, such as arc geometries for RA plans or gantry angles for IMRT plans, was used across all patients in the cohort. To achieve 95% of the dose to 95% of the PTV volume, all plans underwent multiple optimization iterations.

In vertex plans, specific objectives were set for the HD vertices and the two avoidance shells. Two shells, Shell 1 and Shell 2, were designed to optimize dose distribution in the HD vertices and ensure rapid dose fall-off, reducing exposure to nearby tissues and organs. Shell 1 has an outer radius of 0.5 cm and an inner radius of 0.2 cm, while Shell 2 has an outer radius of 0.8 cm and an inner radius of 0.5 cm.

The plan sum option in the Eclipse treatment planning system was used to determine the cumulative dose distribution for both plans. The cumulative dose distribution from both the vertex plans and the plans for the entire PTV was designed to achieve 95% coverage and organ sparing according to defined recommendations for all techniques [8-11].

Dose fall off index

The efficacy of vertex RA plans, seven-field IMRT plans, and nine-field IMRT plans were evaluated for the extent of dose fall-off. The dose fall-off in vertex plans was estimated by calculating the mean doses of the structures created using 16 equally spaced point contours. Each of these contours had a volume of 0.5cc and was located at specific distances from the edge of the target contour (HD vertices) in the central plane of the structure. The contours were named as m_1, m_2, m_3 and m_4 and the distances from the edge of the target contour were 1.5cm (m_1), 2.5cm (m_2), 3.5cm (m_3), and 4.5cm (m_4). Figure 1 illustrates the positions of 16 points, situated at the intersections of lines and concentric circles, as well as the locations of points in the central plane of HD vertices, depicted in a three-dimensional view of the patient's CT.

A tool called normalized dose fall-off index (ʌ) introduced was used to compare the extent of dose fall-off among the three techniques. ʌ was calculated by dividing the mean doses obtained for all four contours by the mean dose obtained for Rapid Arc (RA) plans at the specific distance (1.5 cm) from the central plane of the HD vertices.

$$\Lambda = \frac{Mean\ dose\ to\ m_n}{Mean\ dose\ to\ m_{1(Rapid\ arc)}} \qquad \text{Equation 1}$$

Where, m_n is the dose fall off analysis structure name in any of three composite plans and n varies from 1 to 4 representing structures at incremental distances from 1.5cm to 4.5cm. This normalization allows for a comparison of the dose fall-off characteristics between different treatment techniques and represents the relative dose fall-off for each treatment technique in comparison to the reference RA plans. A value greater than 1 indicates a slower decrease in dose compared to the RA plans, while a value less than 1 indicates a faster dose decrease than the RA plans. To obtain the ʌ index for each technique (RA, seven-field IMRT, and nine-field IMRT), normalized values were averaged over the cohort of patients. This

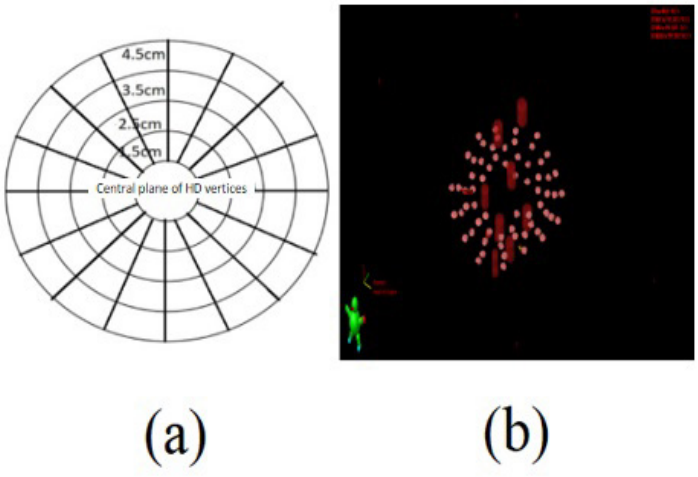

Figure 1. a, depicts the positions of 16 points, situated at the intersections of lines and concentric circles in a diagrammatic fashion. b, shows the locations of points in the central plane of HD vertices, depicted in a three-dimensional view of the patient's CT

provides a representative measure of the average dose fall-off behavior for each treatment technique across the patient population studied.

Valley dose percentage

To obtain the valley dose percentage relative to the prescription dose for all three techniques, 15 dose profiles were generated. These profiles were created using dose profile tool in Eclipse Treatment Planning System (Varian) by selecting points along the linear distance between two HD vertices in multiple planes. This process was repeated for different combinations of HD vertex contour pairs in each plan. The lowest dose at the midpoint of the CTC separation was noted as the valley dose. A total of 675 line dose profiles were obtained to determine the average percentage of valley dose across the three techniques. The valley doses falling within specific class intervals of CTC were grouped together and averaged to analyze the variation of valley dose percentage with respect to CTC. To visualize the data, a graph was plotted with the lower limit of the CTC intervals on the x-axis and the corresponding percentage of valley doses on the y-axis. The curve fitting techniques, including both linear and quadratic equations, were applied to the data using Microsoft Excel. This approach enabled a precise quantification of the relationship between CTC intervals and valley dose percentages.

Results

Dose fall off index

The dose fall-off values beyond HD vertices at different distances from the vertex in the central plane for three treatment techniques: Rapid Arc, seven-field IMRT, and nine-field IMRT fields are as shown in Figure 2. The ʌ values have been standardized by comparing them to the mean dose received by a contour containing sixteen evenly spaced point contours within the rapid arc plans, situated at a distance of 1.5 cm from the central plane of the HD vertices.

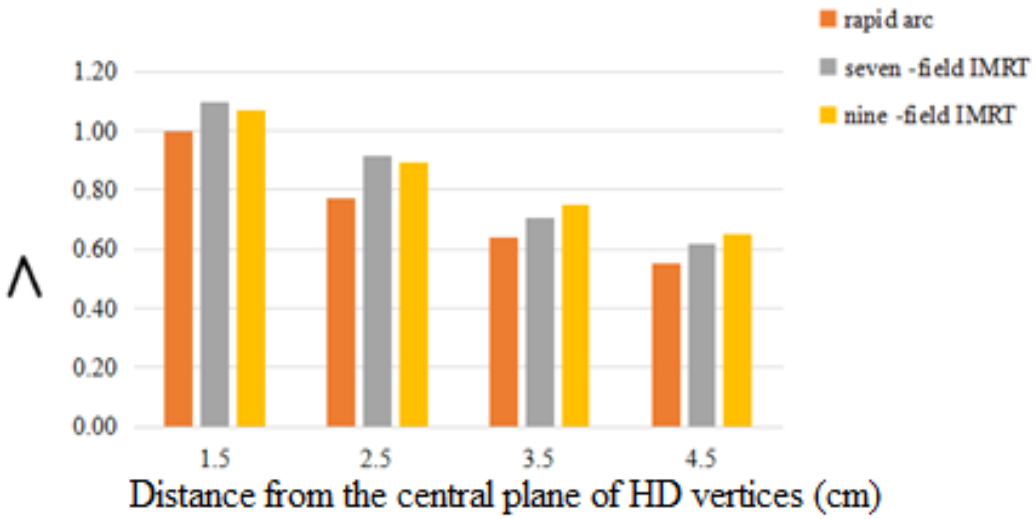

Figure 2. The Column Plot Illustrates Dose Reduction Beyond High-Dose Vertices, with ʌ Values Standardized to the Mean Dose of 16 Evenly Spaced Points 1.5 cm from the Central Plane in Rapid arc Plans.

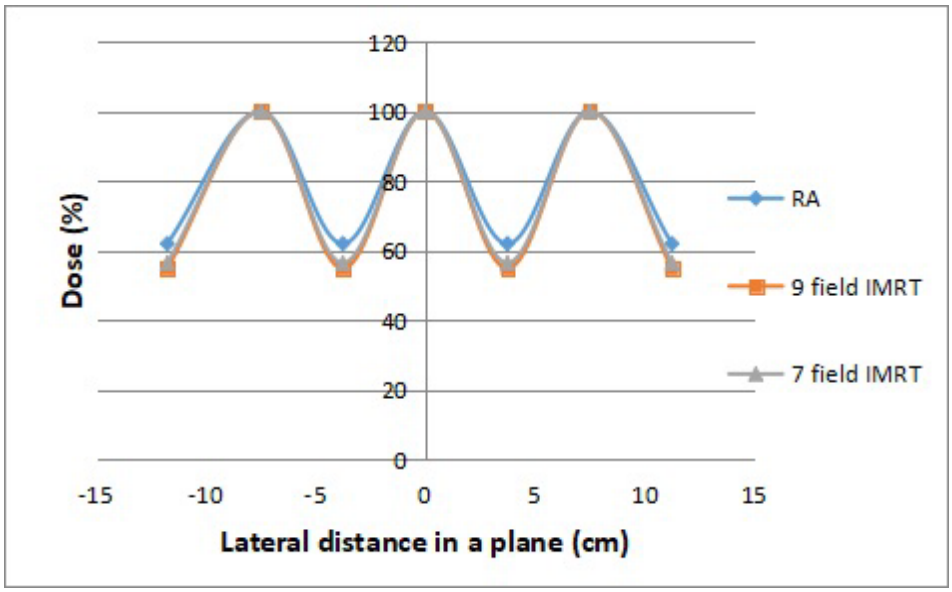

Figure 3. The Graph Represents the Variation of Valley Dose for Rapid arc (RA), 9 field IMRT and 7 Field IMRT with Respect to the Average CTC

As the distance increased further away from the central plane of HD vertex contour, the dose fall-off values decreased for all three treatment techniques. RA demonstrates the steepest dose fall-off, indicated by lower values compared to seven-field IMRT and nine-field IMRT at each distance. Between seven-field IMRT and nine-field IMRT, the dose fall-off values were similar, with slightly higher values observed for seven-field IMRT.

Valley dose percentage

The average CTC obtained for the cohort of patient was 3.75cm and the percentage valley doses obtained were 62.05%, 55.02% and 56.56% for RA, nine-field IMRT and seven-field IMRT plans respectively. Figure 3 represents the variation of valley and peak doses for all the three techniques.

The Table 1 presents a comparison of valley doses across different CTC class intervals for three different radiation therapy techniques: RA, nine-field IMRT, and seven-field IMRT. When CTC is small valley doses are similar across all the three techniques and when CTC increases there is a noticeable difference in the valley dose among the three techniques.

Figure 4 shows the graph illustrating the relationship between average valley dose percentage and center-to-center spacing (CTC) for RA, 9-field IMRT, and 7-field IMRT, with trendlines inserted to highlight the observed trends.

The equation obtained to quantify the valley doses with respect to the techniques employed for various CTC class intervals is:

$$\text{Valley dose percentage} = a_1 (CTC)^2 + a_2 (CTC) + a_3 \quad \text{Equation 2}$$

Where the coefficients a_1, a_2 and a_3 are determined from the curve fitting data and are tabulated in Table 2.

Table 1. The Data Generated from the Dose Profiles for the Cohort of Patients were Grouped within Class Intervals of Center to Center Spacing (CTC). Average valley dose percentage for a particular class interval was tabulated for rapid arc, 9 field IMRT and 7- field IMRT

Class Interval CTC(cm)	Valley dose percentage		
	Rapid Arc	9 field IMRT	7 field IMRT
2.0-2.5	80.29	79.72	79.82
2.5-3.0	78.41	68.23	72.47
3.0-3.5	69.51	62.3	66.61
4.0-4.5	62.36	56.52	56.45
5.0-5.5	51.28	49.14	53.46

Discussion

The heterogeneous delivery of dose distribution in LRT helps reduce hypoxia and improve therapeutic outcomes [12]. Our study focused on the dose fall index and valley doses for various treatment techniques.

Dose fall off index

The dose fall of index Λ provides a quantitative measure of dose fall-off. The column plot in Figure 2 visually represents the reduction in dose levels beyond the high-dose vertices at designated distances from the central plane of HD vertices. At a distance of 1.5 cm from the central plane of the HD vertices, the Λ index for the RA plans was 1.00, indicating a relatively steep dose

Table 2. The Coefficients of the Quadratic Equation to Compute the Valley Doses for Rapid arc, Nine Field IMRT and Seven-Field IMRT

Techniques	a_1	a_2	a_3
Rapid Arc	0	-9.851	100.88
9 field IMRT	2.6301	-27.777	123.15
7 field IMRT	2.5493	-26.783	123.43

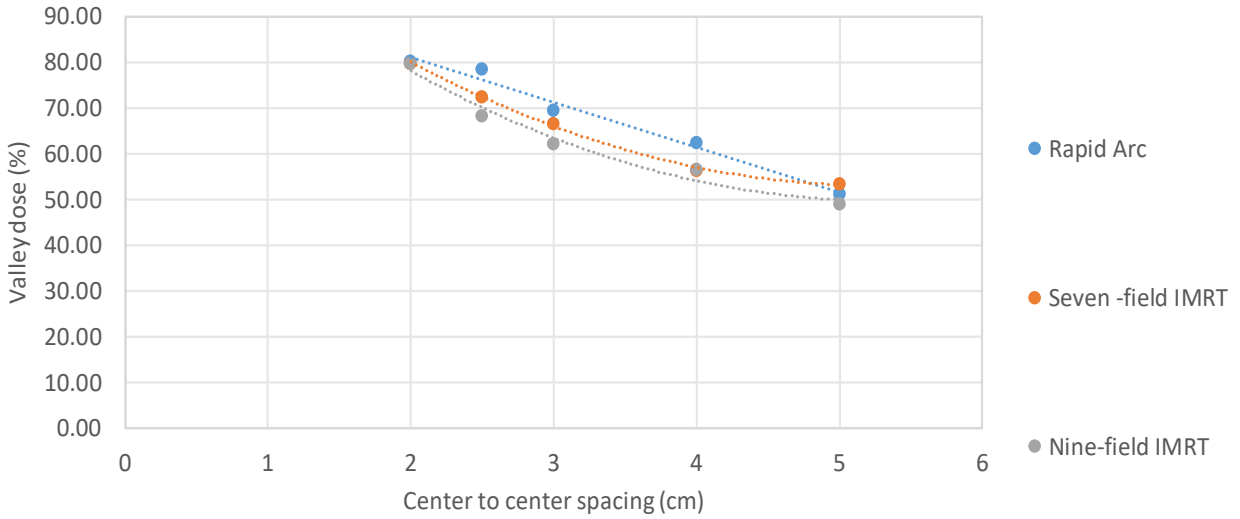

Figure 4. The Graph Shows the Variation of Valley Dose Percentage with Changes in Center-to-Center Spacing (CTC)

fall-off. For the seven-field IMRT technique, the Λ index was 1.10, whereas for the nine-field IMRT technique, it was 1.06. Lower Λ indices indicated a more rapid dose fall-off with increasing distance from the central plane. At greater distances of 3.5 cm and 4.5 cm, there was a noticeable change in the pattern of dose fall-off between the seven-field IMRT and nine-field IMRT plans. The nine-field IMRT plans exhibited higher Λ values compared to the seven-field IMRT plans, which can be attributed to the increased number of fields arranged in close proximity in the nine-field technique, contributing to higher doses in these regions in nine-field IMRT than that in the seven-field IMRT plans. On the other hand, the RA plans demonstrated a consistently steeper dose fall-off at all distances compared to both IMRT techniques. This can be due to the inherent properties of good plan optimization in the RA technique, which enables more precise and conformal dose delivery [13, 14]. The use of the RA technique in creating treatment plans helps achieve a good dose gradient beyond the target areas, leading to effective dose fall-off and thereby reducing the dose to normal tissues. The ʌ index helps in comparing the rate of dose decrease beyond the treatment area between different treatment techniques. It enabled the assessment of the relative effectiveness of each technique in achieving the desired dose distribution and minimizing the dose to normal tissues. Damodar et.al in their study in 2020s suggested employing a unique cross-fire technique utilizing MLCs with the goal of minimizing the radiation exposure to healthy tissues. This approach involved positioning the entry and exit points of the radiation beams symmetrically opposite to each other. Nevertheless, this technique led to the formation of cylindrical regions with elevated radiation doses and exposed nearby healthy tissues to high radiation levels approaching the prescribed dose of 20 Gy [15]. In contrast, spherical dose distribution effectively achieves a lower dose gradient and minimizes doses beyond the target area. Even more, creation of spherical shaped dose distributions is easier to achieve with the help of contoured HD vertex volumes.The use of HD vertices and adoption of RA technique can thus be useful to increase the popularity of SFRT treatment in routine clinical practice and inspire further researches that will help in the correlation of "the actual dosimetric parameters" that affects "the clinical results".

Valley dose percentage

Our study indicates that RA plans deliver a higher average percentage of valley doses compared to IMRT plans. Among the IMRT plans, the difference in valley doses between the nine-field and seven-field configurations is marginal. Thus increasing the number of beam angles in the case of IMRT has minimal impact on the valley dose percentage. In grid therapy, it is imperative to minimize valley doses to as low as 25-30% of the peak doses to enhance therapeutic effectiveness and reduce potential adverse effects. However, the use of multileaf collimators (MLCs) complicates achieving such low valley doses due to inherent interleaf and intraleaf transmissions, as well as beam delivery across multiple gantry angles. This limitation should be considered by centers planning to implement grid therapy. Our study provides a reference for institutions looking to adopt grid therapy, emphasizing the necessity of adjusting peak doses according to clinical needs. Our study reveals that rapid arc plans employs a linear change in valley doses with respect to CTC, while IMRT plans exhibit a quadratic change in valley dose with change in CTC. Treatment technique, CTC, and peak doses can be planned accordingly using equations derived from our study. While reducing valley doses is challenging, these doses can be effectively utilized in LRT, where the entire planning target volume (PTV) is irradiated simultaneously with conventional fractionation.

In conclusions, our study demonstrates that RA plans achieve a steeper dose fall-off and higher average percentage of valley doses compared to IMRT plans, making them more effective for pelvic LRT by minimizing normal tissue exposure. IMRT plans achieve better valley dose reduction because of the restricted angles of the beam's eye view help limit dose spread. On the other hand, rapid arc plans, which use multiple beam angles, offer improved high-dose conformity and sharper dose fall-off.

However, this wider range of beam angles also makes it more challenging to control and reduce valley doses effectively compared to IMRT. The minimal difference in valley doses between the nine-field and seven-field IMRT configurations suggests that the number of beam angles has a limited impact on valley dose percentage. These findings provide valuable insights for optimizing treatment planning and highlight the need for further research to correlate dosimetric parameters with clinical outcomes.

Author Contribution Statement

Both the authors contributed to the conception or design of the work, collected data, analyzed and interpreted the data and wrote manuscript also both are involved in revising the manuscript critically for important intellectual content and to approve the final version to be submitted for publication

Acknowledgements

General

Authors express their thanks to the editors of journal and reviewers for considering the manuscript.

If it was approved by any scientific body/ if it is part of an approved student thesis

Not Applicable, it will be a part of thesis

Ethical Declaration

The study do not require approval from ethical committee as it was a dosimetric study on scans of already treated patients. No humans were involved in the study

Conflict of Interest

Authors declare that there are no conflict of interests

References

1. Bhagyalakshmi AT, Velayudham R. Assessing dosimetric advancements in spatially fractionated radiotherapy: From grids to lattices. Med Dosim. 2024;49(3):206-214. https://doi.org/10.1016/j.meddos.2023.12.003
2. Mohiuddin M, Fujita M, Regine WF, Megooni AS, Ibbott GS, Ahmed MM. High-dose spatially-fractionated radiation (GRID): a new paradigm in the management of advanced cancers. Int J Radiat Oncol Biol Phys. 1999;45(3):721-7. https://doi.org/10.1016/S0360-3016(99)00170-4
3. Wu X, Ahmed MM, Wright J, Gupta S, Pollack A, Ahmed MM. On modern technical approaches of three-dimensional high-dose lattice radiotherapy (LRT). Cureus. 2010;2(3).
4. Zwicker RD, Meigooni A, Mohiuddin M. Therapeutic advantage of grid irradiation for large single fractions. Int J Radiat Oncol Biol Phys. 2004;58(4):1309-15. https://doi.org/10.1016/j.ijrobp.2003.07.003
5. Pellizzon AC. Lattice radiation therapy–its concept and impact in the immunomodulation cancer treatment era. Rev Assoc Med Bras. 2020;66(6):728-31. https://doi.org/10.1590/1806-9282.66.6.728
6. Kanagavelu S, Gupta S, Wu X, Philip S, Wattenberg MM, Hodge JW, et al. In vivo effects of lattice radiation therapy on local and distant lung cancer: potential role of immunomodulation. Radiat Res. 2014;182(2):149-62. https://doi.org/10.1667/RR3819.1
7. Murphy NL, Philip R, Wozniak M, Lee BH, Donnelly ED, Zhang HA. simple dosimetric approach to spatially fractionated GRID radiation therapy using the multileaf collimator for treatment of breast cancers in the prone position. J Appl Clin Med Phys. 2020;21(11):105-14. https://doi.org/10.1002/acm2.13040
8. Bisello S, Cilla S, Benini A, Cardano R, Nguyen NP, Deodato F, et al. Dose–volume constraints for oRganS At risk In Radiotherapy (CORSAIR): an "All-in-One" multicenter–multidisciplinary practical summary. Curr Oncol. 2022;29(10):7021-50. https://doi.org/10.3390/curroncol29100552
9. Emami B. Tolerance of normal tissue to therapeutic radiation. Reports of radiotherapy and Oncology. 2013;1(1):123-7. https://brieflands.com/articles/rro-2782.pdf
10. Lukka HR, Pugh SL, Bruner DW, Bahary JP, Lawton CA, Efstathiou JA, et al. Patient reported outcomes in NRG Oncology RTOG 0938, evaluating two ultrahypofractionated regimens for prostate cancer. Int J Radiat Oncol Biol Phys. 2018;102(2):287-95. https://doi.org/10.1016/j.ijrobp.2018.06.008
11. Bentzen SM, Constine LS, Deasy JO, Eisbruch A, Jackson A, Marks LB, et al. Quantitative Analyses of Normal Tissue Effects in the Clinic (QUANTEC): an introduction to the scientific issues. Int J Radiat Oncol Biol Phys. 2010;76(3):S3-9. https://doi.org/10.1016/j.ijrobp.2009.09.040
12. Ferini G, Valenti V, Tripoli A, Illari SI, Molino L, Parisi S, et al. Lattice or oxygen-guided radiotherapy: what if they converge? Possible future directions in the era of immunotherapy. Cancers. 2021;13:3290. https://doi.org/10.3390/cancers13133290
13. Iori F, Cappelli A, D'Angelo E, Cozzi S, Ghersi SF, De Felice F, et al. Lattice Radiation Therapy in clinical practice: A systematic review. Clin Transl Radiat Oncol. 2023;39:100569. https://doi.org/10.1016/j.ctro.2022.100569
14. Oliver M, Ansbacher W, Beckham WA. Comparing planning time, delivery time and plan quality for IMRT, RapidArc and Tomotherapy. J Appl Clin Med Phys. 2009;10(4):117-31. https://doi.org/10.1120/jacmp.v10i4.3068
15. Pokhrel D, Halfman M, Sanford L, Chen Q, Kudrimoti M. A novel, yet simple MLC-based 3D-crossfire technique for spatially fractionated GRID therapy treatment of deep-seated bulky tumors. J Appl Clin Med Phys. 2020;21(3):68-74. https://doi.org/10.1002/acm2.12826